JOURNAL OF VIROLOGY, Mar. 2011, p. 2781–2792 Vol. 85, No. 6
0022-538X/11/$12.00 doi:10.1128/JVI.01631-10

Rotavirus Replication Requires a Functional Proteasome for Effective Assembly of Viroplasms[▽]

R. Contin,[1]†# F. Arnoldi,[1,2]† M. Mano,[1] and O. R. Burrone[1]*

International Centre for Genetic Engineering and Biotechnology (ICGEB), Padriciano 99, 34149 Trieste, Italy,[1] and Dipartimento Universitario Clinico di Biomedicina, Università degli Studi di Trieste, Trieste, Italy[2]

Received 4 August 2010/Accepted 22 December 2010

The ubiquitin-proteasome system has been shown to play an important role in the replication cycle of different viruses. In this study, we describe a strong impairment of rotavirus replication upon inhibition of proteasomal activity. The effect was evidenced at the level of accumulation of viral proteins, viral RNA, and yield of infective particles. Kinetic studies revealed that the early steps of the replicative cycle following attachment, entry, and uncoating were clearly more sensitive to proteasome inhibition. We ruled out a direct inhibition of the viral polymerase activities and stability of viral proteins and found that the crucial step that was impaired by blocking proteasome activity was the assembly of new viroplasms. This was demonstrated by using chemical inhibitors of proteasome and by gene silencing using small interfering RNAs (siRNAs) specific for different proteasomal subunits and for the ubiquitin precursor RPS27A. In addition, we show that the effect of proteasome inhibition on virus infection is not due to increased levels of beta interferon (IFN-β).

Rotavirus is a nonenveloped double-stranded RNA (dsRNA) virus that belongs to the family *Reoviridae* and is an important cause of acute gastroenteritis in infants and young children. The infectious mature viral particle is composed of three concentric layers of proteins (triple-layered particle [TLP]) that surround the 11 segments of double-stranded RNA of the viral genome (43, 57). The outer layer consists of the spike protein VP4 and the glycoprotein VP7, while the intermediate and internal layers are made up of VP6 and VP2, respectively. Associated with the internal layer VP2 are the segmented genome and complexes of the viral RNA-dependent RNA polymerase (RdRP) VP1 with the RNA-capping enzyme VP3. The viral genome encodes six structural proteins (VP1 to VP4, VP6, VP7) and, depending on the viral strain, five or six nonstructural proteins (NSP1 to NSP6) that are expressed during the virus replicative cycle (17).

Entry of the virus into the host cell is associated with the loss of the VP4-VP7 outer layer converting the TLP into a double-layered particle (DLP), which becomes transcriptionally active, producing plus-strand RNAs (mRNAs) (35, 53). The 11 viral mRNAs are 5′ capped but nonpolyadenylated, and upon release into the cytoplasm, they are translated into viral proteins. Plus-strand RNAs also serve as template for the synthesis of the new dsRNA genome segments. At early time points postinfection, electron-dense structures, named viroplasms, appear in the cytoplasm of infected cells. These are the structures where synthesis of dsRNA (genome replication) and the initial steps of assembly of new particles take place (3, 16, 42). Several viral proteins have been shown to accumulate in viroplasms during rotavirus infection. In particular, two nonstructural proteins, NSP5 and NSP2, that localize in viroplasms of infected cells were found to be essential for viroplasm formation, dsRNA synthesis, and virus replication (8, 38, 52, 55). Also, some structural proteins, such as VP1, VP2, VP3, and VP6, localize in viroplasms of infected cells (17). Newly assembled DLPs, through interaction with NSP4, bud into the lumen of the endoplasmic reticulum, acquiring a transient envelope, which is later replaced with the VP4-VP7 layer (17). Release of mature viral particles from the cell occurs either by cell lysis or by a nonclassical, Golgi apparatus-independent, vesicular transport pathway (12, 17, 37).

The cellular ubiquitin-proteasome system (UPS) is an elaborate machinery that recognizes and degrades polyubiquitinylated proteins. Its main function is to degrade misfolded, damaged, or unneeded proteins. However, UPS has also been shown to finely regulate different cellular processes, including gene transcription, signal transduction, cell cycle progression, apoptosis, and DNA repair (32). Structurally, the proteasome consists of two main complexes: the 20S proteolytic core (core particle [CP]) and the 19S regulatory particle (RP), which together form the 26S proteasome. In order to be recognized for degradation, substrates need to be tagged with a polyubiquitin chain of at least four units (21). This process occurs by the sequential action of three enzymes: the ubiquitin-activating enzyme E1, which activates ubiquitin molecules in its active center, the ubiquitin conjugation enzyme E2, which transfers activated ubiquitin from E1 to E3, which in turn ubiquitinylates the target. The recognition of the ubiquitinylated substrates is mediated by the 19S RP subunit, while the hydrolysis of the targeted proteins occurs in the narrow channel of the 20S CP, producing a heterogeneous mixture of peptides (32).

Many studies have demonstrated that different types of virus manipulate the ubiquitin-proteasome pathway in order to evade cellular responses and enhance viral replication (31, 47). In this work, we show that a functional proteasome is required

* Corresponding author. Mailing address: International Centre for Genetic Engineering and Biotechnology (ICGEB), Padriciano 99, 34149 Trieste, Italy. Phone: 39-040-3757314. Fax: 39-040-226555. E-mail: burrone@icgeb.org.

† These authors have contributed equally.

Present address: Centro di Medicina Rigenerativa, Dipartimento di Scienze Biomediche, Università degli Studi di Modena e Reggio Emilia, Italy.

▽ Published ahead of print on 12 January 2011.

for rotavirus in order to establish a productive replication cycle.

MATERIALS AND METHODS

Cells, viruses, and reagents. MA104 cells (embryonic African green monkey kidney cells) were grown as monolayers in Dulbecco's modified Eagle's medium (DMEM) containing 10% fetal calf serum (FCS; Invitrogen), 2 mM L-glutamine, and 50 μg/ml gentamicin (Invitrogen).

C7-MA104 clone and the NSP5-enhanced green fluorescent protein (EGFP)/MA104 cell line were obtained as previously described (2, 14) and cultured in complete DMEM supplemented with 800 μg/ml Geneticin (G-418; Gibco BRL).

The BSR-T7/5 cell line, a kind gift of Karl Conzelmann, was cultured in DMEM complete with high glucose supplemented with 1 mg/ml Geneticin (G-418; Gibco BRL).

Simian SA11 (G3, P6[1]) and porcine OSU (G5, P9[7]) rotavirus strains were propagated in MA104 cells, as described previously (18, 28).

MG132 (Calbiochem), lactacystin (Sigma), and bortezomib (Selleck Chemicals) were dissolved in dimethyl sulfoxide (DMSO) at a final concentration of 50 μM.

Plasmids. pT_7v-NSP5, pT_7v-NSP2, pcDNA3-SV5-VP1 (encoding tag-VP1), pcDNA3-VP2, and pcDNA3-VP6 were obtained as previously described (4, 10, 15, 19). The NSP5 gene was derived from the OSU rotavirus strain, and the NSP2, VP1, VP2 and VP6 genes came from the SA11 strain.

In order to construct the plasmid pVAX-T7-segment11-ribo-T7stop, indicated in the Results section as pVAX-segment 11, the pVAX vector (Invitrogen) was modified by deletion of the cytomegalovirus (CMV) promoter using NdeI and ApaI restriction enzymes and subsequent insertion of an oligonucleotide containing the XmaI, ApaI, and SacII restriction sites (5′-TATGGGTACCTACTCCCGGGTTACAGGGCCCGCGGAGGCC-3′; Sigma). Between the sites of XmaI and ApaI, a synthetic sequence (Genscript) has been inserted in order to clone the ribozyme and the T7 terminator (5′-ccCGGGTCGGCATGGCATCTCCACCTCCTCGCGGTCCGACCTGGGCATCCGAAGGAGGACGTCGTCCACTCGGATGGCTAAGGGAGAGCTcggatccGGCTGCTAACAAAGCCCGAAAGGAAGCTGAGTTGGCTGCTGCCACCGCTGAGCAATAACTAGCATAACCCCTTGGGGCCTCTAAACGGGTCTTGAGGGGTTTTTTGCTGAAAGGAGGAACTATATCCGGATCGAGATCCtctagagggccc-3′; capital letters indicate the ribozyme, and the T7 terminator and the XmaI and ApaI sites are underlined). The SA11 segment has been amplified from the corresponding cDNA with the following primers: 5′-AGGTACCTAATACGACTCACTATAGGCTTTTAAAGCGCTACAG-3′ and 5′-GACCGGTCACATAACTGGAGTGGGGA-3′ (Sigma). The forward primer has been designed with the T7 promoter upstream of the initial nucleotides of the 5′ untranslated region (UTR) of the rotavirus genomic fragment. The amplified sequence has been inserted between KpnI and XmaI sites to obtain the pVAX-T7-segment11-ribo-T7stop plasmid.

Transient transfections. For transfection experiments, subconfluent monolayers of MA104 cells in six-well plates (Falcon) were infected with T7-recombinant vaccinia virus (strain vTF7.3 [23]) to increase the expression level of proteins encoded by the transfected plasmids. One hour later, cells were transfected with a maximum of 4 μg/well of total plasmid DNA using Lipofectamine 2000 (Gibco BRL) according to the manufacturer's instructions. The relative amounts of plasmids were opportunely adjusted as previously described (10). Transfected cells were harvested at 24 h posttransfection, after 4 h of proteasome inhibitor (MG132, 50 μM) or DMSO treatment. Transfections of pVAX and pcDNA3-NSP5 plasmids were performed in BSR T7-5 cells using Lipofectamine 2000 and 6 μg/well of plasmid DNA, without T7-recombinant vaccinia virus infection. Transfected cells were harvested at 24 h posttransfection, after 4 h of treatment with proteasome inhibitor (MG132, 25 μM) or DMSO.

Cellular extracts (corresponding to about 5×10^5 cells) were prepared in boiling Laemmli sample buffer and were subsequently sonicated and centrifuged at 2, 000 × *g* for 5 min at 4°C. Portions (10 μl) of supernatants were separated by polyacrylamide gel electrophoresis (PAGE) and analyzed by Western immunoblotting.

SDS-PAGE and Western immunoblot analysis. Cellular extracts were resolved through 12% SDS-PAGE and, after electrophoresis, transferred to polyvinylidene difluoride (PVDF) membranes (Millipore). The membranes were incubated with the following antibodies: anti-NSP2 mouse serum (1:3,000), anti-NSP5 guinea pig serum (1:10,000), anti-VP2 mouse serum (1:5,000), monoclonal mouse anti-p53 (1:5,000; Santa Cruz Biotechnology), monoclonal mouse anti-IRF3 (1:200; Santa Cruz Biotechnology), polyclonal rabbit anti-PSMC6 (1:500; Abcam), rabbit anti-actin (1:500; Sigma), and peroxidase-conjugated goat anti-guinea pig (1:10,000; Jackson ImmunoResearch), goat anti-mouse (1:5,000; Jackson ImmunoResearch), and goat anti-rabbit (1:5,000; Thermo Scientific) secondary antibodies. Signals were detected by using the enhanced chemiluminescence (ECL) system (Pierce). Sera were produced by immunization of guinea pigs and mice as described previously (1, 4, 25).

Virus titration. MA104 cells were infected in the presence or in the absence of proteasome inhibitors. At 7 h postinfection (p.i.) viral particles in the supernatant of infected cells were purified and used to infect NSP5-EGFP cells in a 96-well plate at different dilutions. Virus titer was determined as fluorescence-forming units (FFU) in the NSP5-EGFP/MA104 cell line, as previously described (8).

Immunofluorescence microscopy. Immunofluorescence experiments were performed as described previously (15) with anti-NSP2 mouse serum (1:200) and anti-VP2 mouse serum (1:500) and with anti-NSP2 guinea pig serum (1:200), rhodamine isothiocyanate-conjugated goat anti-mouse antibody (1:200; Jackson ImmunoResearch), and Alexa Fluor 647-conjugated goat anti-guinea pig antibody (1:1,000; Invitrogen; fluorescence shown in purple) as secondary antibodies. Samples were analyzed by confocal microscopy (Zeiss LSM510 equipped with a 100× numerical aperture [NA] 1.3 objective or Zeiss LSM510 Meta equipped with a 63× NA 1.4 objective).

Quantification of viroplasms was performed at the ICGEB High-Throughput Screening Facility (http://www.icgeb.org/high-throughput-screening.html). Image acquisition was performed using an ImageXpress Micro automated high-content screening microscope (Molecular Devices) equipped with a 20× objective; a total of 16 fields were acquired from each well, which corresponds to an average of ca. 1,000 cells imaged and analyzed per experimental condition and replicate. Automated image analysis of viroplasm formation was performed in MetaXpress software (Molecular Devices) using the Transfluor application module, which identifies cell nuclei (blue channel) and subsequently quantifies the FFU for virus titration or the number of viroplasms present in each cell (green channel).

siRNA transfection. Pools of four different small interfering RNAs (siRNAs) per gene target (Dharmacon, 50 nM final concentration) were transfected in 96-well plates (for Western blotting) or 384-well plates (for fluorescence microscopy) with Lipofectamine RNAiMax (Invitrogen; 0.9 μl/well), using a reverse transfection protocol. At 48 h after siRNA transfection, cells were washed three times in serum-free medium and virus was added to the relevant wells; at 6 h postinfection, the cells were processed for Western blotting as described above or stained with Hoechst 33342 for automated quantification of viroplasms by fluorescence microscopy.

***In vitro* DLP transcription assays.** DLPs purified by CsCl gradient centrifugation were incubated with 5× transcription buffer (Promega), 3 μM dithiothreitol (DTT), 3 μM ATP, CTP, and GTP, 0.3 μM UTP (Fermentas), and [α-P^{32}]UTP (Perkin Elmer), 40 U RNasin (Promega) and DMSO (control), or 50 μM MG132. The transcription mix was incubated 3 to 4 h at 42°C and ultracentrifuged in a Airfuge ultracentrifuge (Beckman Coulter) at 40,000 rpm for 1 h. Supernatants were treated with 1 μg/μl proteinase K (Invitrogen) for 30 min at 37°C, spotted on a PVDF membrane, previously treated with 10% trichloroacetic acid (TCA), and washed several times with 10% TCA. Membranes were imaged with Instant Imager instrument (Packard), and quantification of counts per minute was performed with Imager software.

[^{35}S]methionine labeling. For *in vivo* [^{35}S]methionine labeling of rotavirus proteins, confluent monolayers of MA104 cells in six-well plates (Falcon) were infected with SA11 (G3, P6[1]) and OSU (G5, P9[7]) rotavirus strains at a multiplicity of infection (MOI) of 3 for 1 h at 37°C. Cells were extensively washed with PBS and incubated for 1 h with methionine-free DMEM (GIBCO Invitrogen). Then, methionine-free DMEM containing 20 μCi/ml [^{35}S]methionine (Amersham), 10 μM MG132, or equal volumes of DMSO was added to the samples at different times postinfection (1.5, 3.0, 4.5 h p.i.). After 30 min of labeling, cells were lysed in boiling Laemmli sample buffer and lysates were separated by 12% SDS-PAGE.

***In vivo* phosphorylation with $^{32}P_i$.** For *in vivo* phosphorylation assays, confluent monolayers of MA104 cells in six-well plates (Falcon) were infected with rotavirus at an MOI of 3 for 1 h at 37°C, and after 1 h, medium containing virus was replaced with serum-free DMEM. At 4 h postinfection, cells were extensively washed and maintained in phosphate-free DMEM (GIBCO, Invitrogen) for 1 h. At 5 h p.i., the medium was adjusted to 10 μg/ml of actinomycin D, 10 μM MG132, or DMSO, 100 μM each nucleosides (adenosine, cytidine, guanosine, uridine; Sigma), and 100 μCi/ml of $^{32}P_i$ (Perkin Elmer). At 7 h p.i., the cells were lysed with three cycles of freeze-thawing and the lysates were centrifuged. Supernatants were incubated for 30 min with proteinase K (Invitrogen), and dsRNA was extracted with phenol-chloroform and ethanol precipitation. Resuspended dsRNA was electrophoresed in a 12% SDS-PAGE gel for 8 h at 30 mA.

Real-time PCR. For analysis of the expression of rotavirus NSP5, cellular IFN-β, and GAPDH, confluent monolayers of MA104 cells in six-well plates (Falcon) were infected with SA11 (G3, P6[1]) and OSU (G5, P9[7]) rotavirus

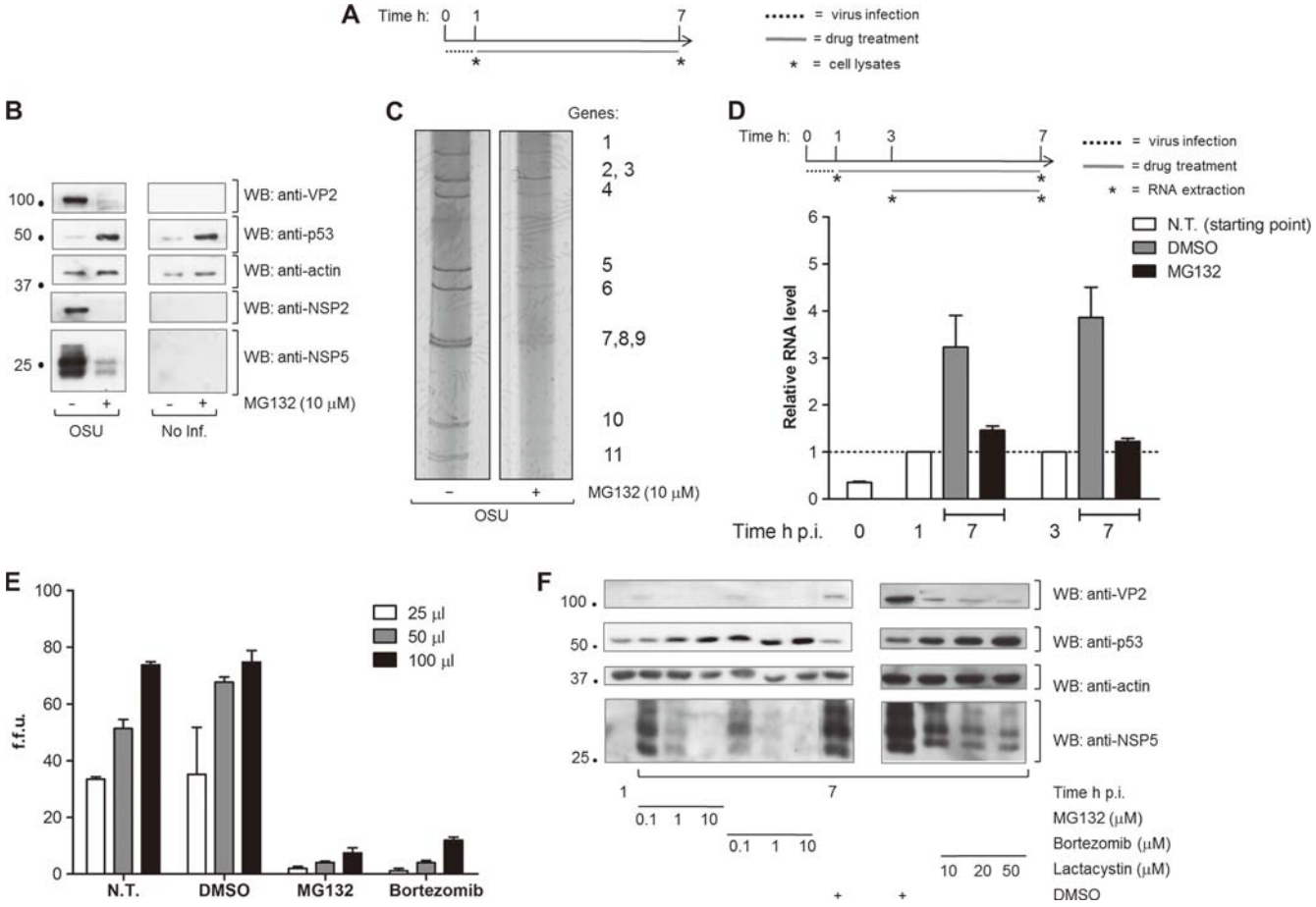

FIG. 1. Effect of proteasome inhibition on rotavirus replication. (A) Schematic representation of the experimental procedure adopted on MA104 cells infected with OSU (MOI, 3) in the experiments described in the legends to panels B, C, E, and F. (B) Western blots of cellular extracts of noninfected (No inf.) and OSU-infected cells with or without MG132 treatment (10 μM), reacted with the indicated antibodies. (C) Silver staining of viral dsRNA from MG132-treated (10 μM) and untreated infected cells (numbers indicate the viral genome segments). (D) Quantitative real-time RT-PCR of segment 11 from total RNA extracted from MG132 (10 μM) or DMSO-treated MA104-infected cells (OSU; MOI, 3). Upper panel, scheme of the experiment; asterisks denote time points at which cell lysates were prepared. Bottom panel, RNA levels relative to the amount determined at the moment of MG132 or DMSO addition. (E) Virus yields expressed as FFU, obtained from nontreated cells (N.T.) or cells treated with the indicated reagents. Quantifications were performed with MetaXpress software as described in Materials and Methods. Graph reports average ± standard error of the mean (SEM) in each column. (F) Western blot of extracts of infected cells treated with different proteasome inhibitors at different concentrations, reacted with the indicated antibodies. p53 was used to monitor proteasome inhibition, and actin was used as a loading control.

strains at an MOI of 3 for 1 h at 37°C. After 1 h or 3 h, the medium containing virus was replaced with DMEM containing 10 μM MG132 or the corresponding volume of DMSO. At 7 h p.i., cells were lysed with three cycles of freeze-thawing and total RNA was extracted as described above.

One-tenth of the volume of the total RNA was retrotranscribed using random hexamers (IDT), and the product of retrotranscription was used as a template for quantitative reverse transcription-PCR (qRT-PCR) using SybrGreen technology (Applied Biosystems) and specific primer sets (IDT) for IFN-β (forward, 5′-AGGACAGGATGAACTTTGAC-3′; reverse, 5′-TGATAGACATTAGCCAGGAG-3′), for rotavirus NSP5 (forward, 5′-ATGTCTCTCAGCATT-3′; reverse, 5′-AGATTTTCCAGAAAGAGT-3′), and for GAPDH (forward, 5′-GGGCGCCTGGTCACCAGGGCTGC-3′; reverse, 5′-GAGCCCCAGCCTTCTCCATGGTGG-3′). All the amplifications were performed on a 7000 ABI Prism instrument (Applied Biosystems). Relative gene expression was normalized to the glutaraldehyde 3-phosphate dehydrogenase (GAPDH) gene according to the formula $2^{-\Delta\Delta C_t}$ ($\Delta\Delta C_t = \Delta C_{t,\text{sample}} - \Delta C_{t,\text{untreated control}}$).

RESULTS

Proteasome inhibition affects early stages of rotavirus infection. In rotavirus-infected cells, treatment with the proteasome inhibitor MG132 caused a strong decrease in the amount of viral proteins accumulated during the virus replication cycle. When infected cells were treated with MG132 (10 μM) after virus adsorption until hour 7 postinfection (p.i.) (Fig. 1A), the accumulation of both structural (VP2) and nonstructural (NSP5, NSP2) rotaviral proteins was strongly affected (Fig. 1B). The effectiveness of MG132 treatment on proteasome activity was confirmed by analysis of the levels of p53 (39), which increased upon proteasome inhibition. As expected, following proteasome inhibition, production of newly replicated genomic viral dsRNA (Fig. 1C), accumulation of viral RNA (represented by RNA levels of segment 11 by qRT-PCR, Fig. 1D), and virus yields (Fig. 1E) were heavily impaired.

Other proteasome inhibitors which have different inhibition mechanisms, such as bortezomib and lactacystin, also had a strong effect on virus replication in parallel with an increase in p53 accumulation (Fig. 1F). We thus concluded that proteasome activity is required for efficient virus replication.

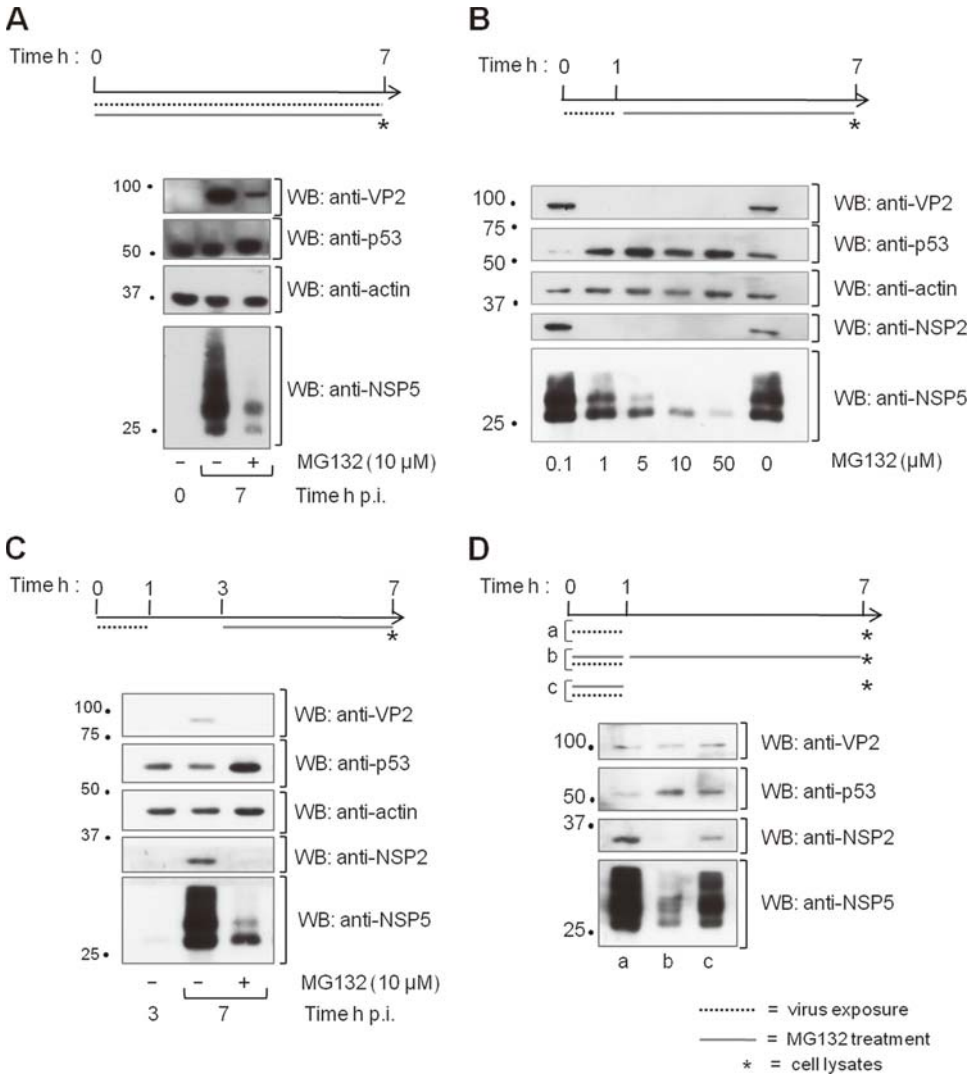

FIG. 2. Kinetics of rotavirus infection and proteasome inhibition. Western blots of MA104 cells infected with OSU (MOI, 3) and treated with MG132 (10 μM) for different times, as indicated. *, specific time point at which cell lysates were prepared. (A) Cells exposed to virus and treated with MG132 for 7 h. (B) Cells exposed to virus for 1 h followed by 6 h of MG132 treatment. (C) Cells exposed to virus for 1 h and treated with MG132 from 3 h to 7 h p.i. (D) Cells exposed to virus for 1 h and not treated (lane a), treated with MG132 during virus exposure and afterwards (lane b), and treated with MG132 only during virus exposure (lane c). Blots were reacted with the indicated antibodies. In all panels, p53 was used to confirm inhibition of the proteasome and actin as a loading control.

In order to investigate whether inhibition of viral replication was due to impairment of early or late events postinfection, we tested the effect of adding MG132 simultaneously with virus (Fig. 2A), after 1 h of virus adsorption and virus entry (Fig. 2B), and at 3 h p.i. (Fig. 2C). In all three cases, strong reduction in viral protein accumulation was observed in an inhibitor concentration-dependent manner (Fig. 2B). Although inhibition of virus replication was particularly sensitive at early time points after infection, the effect observed when inhibitors were added at 3 h p.i. indicates that it did not involve a specific block in the steps of virus entry and uncoating of TLPs. This was further confirmed by adding MG132 for only 1 h, during the steps of virus entrance and uncoating that resulted, as shown in Fig. 2D, in a significant level of virus replication.

Further kinetic experiments were performed to better define the time window within the viral replication cycle in which proteasome activity was required. For this, cells were infected for 1 h and treated with MG132 or bortezomib for 4 h at different times postinfection (Fig. 3A). As shown in Fig. 3B, a more clear arrest on viral protein accumulation was observed when the proteasome inhibitor was added at relatively earlier time points. Indeed, when inhibitors were added at 5 h p.i. or later, the effect was much reduced, suggesting that once the infection was well established with a robust accumulation of viroplasms, the requirement for proteasome activity was less significant. As shown in Fig. 4, the need of proteasomal activity for virus replication was evident in two different rotavirus strains (porcine OSU and monkey SA11).

Proteasome inhibitors do not affect viral polymerase. These results suggest that once infection is well established, rotavirus is able to maintain a normal level of mRNA transcription and

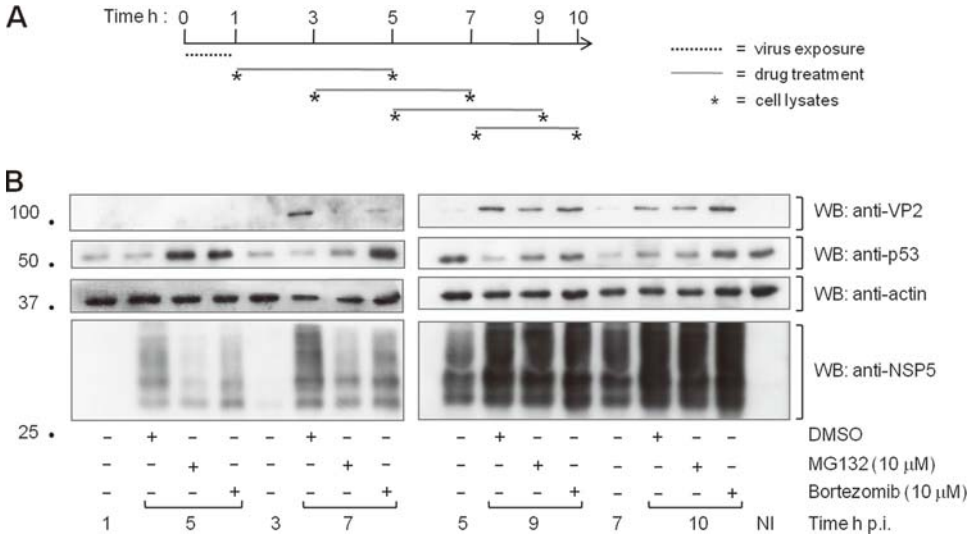

FIG. 3. Time window treatment with proteasome inhibitors. (A) Scheme of the experiment performed with MA104 cells exposed to virus (OSU; MOI, 3) for 1 h and analyzed at the starting point and endpoint of the indicated time window treatments with DMSO, MG132, or bortezomib. *, time point at which cell lysates were prepared. (B) Western blot of cellular lysates derived from cells infected for the indicated time periods and treated with the proteasome inhibitors or DMSO. NI, noninfected cells. Blots were reacted with the indicated antibodies; p53 was used to monitor proteasome inhibition, and actin was used as a loading control.

viral genomic dsRNA synthesis, even when the proteasome is inhibited. We therefore tested whether MG132 had a direct effect on the transcriptase and replicase activities of the VP1 viral polymerase. The transcriptase activity was measured by [α-^{32}P]UTP incorporation into viral mRNAs transcribed *in vitro* from DLPs. As shown in Fig. 5A, no difference was observed in the transcription levels performed in the presence or absence of MG132. The replicase activity was determined *in vivo* by pulse-labeling with $^{32}P_i$ of dsRNA at a time point when high levels of replication take place (5 to 7 h p.i.) (54). The rate of synthesis of dsRNA in virus-infected cells treated with MG132 was comparable to that of nontreated control cells (Fig. 5B). From these experiments we could conclude that proteasome inhibition does not directly affect the viral polymerase activities.

In addition, we found that neither the rate of viral protein synthesis determined at 1.5 h, 3.0 h, or 4.5 h p.i. by a 30-min pulse of [^{35}S]methionine incorporation (Fig. 5C) nor the ability of cells to translate a virus-like mRNA (i.e., containing the 5′ and 3′ UTRs) (Fig. 5D) were affected in the presence of MG132. Moreover, the stability of different viral proteins independently expressed in noninfected cells (NSP5, VP2, NSP2) did not change upon proteasome inhibition. As shown in Fig. 6, this was assessed by transient transfection (i) in MA104 cells driven by T7/vaccinia virus, (ii) in the BSR-T7/5 cell line that stably expresses the T7 RNA polymerase (therefore in the absence of vaccinia virus), and (iii) in the C7-MA104 clone (2) stably expressing NSP5.

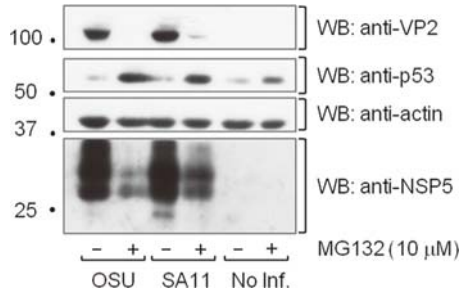

FIG. 4. Effect of proteasome inhibition on different rotavirus strains. Western blot of cellular extracts obtained from OSU- and SA11-infected MA104 cells treated or not treated (No Inf.) with MG132 (10 μM) from 1 h to 7 h p.i. Blots were reacted with the indicated antibodies; p53 was used to monitor proteasome inhibition, and actin was used as a loading control.

Proteasome activity is required for viroplasm formation. The data presented above suggested that the requirement of proteasomal activity was more relevant at early time points p.i., when the rate of viroplasm formation is more pronounced (14). We thus investigated the effect of MG132 and bortezomib on viroplasm formation using the MA104 cell line stably expressing the NSP5-EGFP fusion protein that, upon rotavirus infection, relocalizes to viroplasms (14). Both MG132 and bortezomib induced a significant arrest on the formation of viroplasms, which appeared in reduced number and with smaller size with respect to those in control cells, particularly when added at time points between 1 h and 5 h p.i. (Fig. 7A). In contrast, addition of the inhibitors at 7 h p.i. did not show any effect on the number or size of viroplasms (Fig. 7A). These results indicate that the early/middle phases of viroplasm assembly are the ones more susceptible to proteasome inhibition, since no disassembly was observed. These results were also confirmed by immunofluorescence analysis using either anti-NSP2 or anti-NSP5 antibodies (data not shown). Quantification of the reduction of viroplasm formation by proteasome inhibitors was performed by automated image analysis using a high-content screening microscope (Molecular Devices; see Materials and Methods). As shown in Fig. 7B, the number of viroplasms per cell in cells treated for 4 h with MG132 or bortezomib was almost the same as that found in cells fixed at

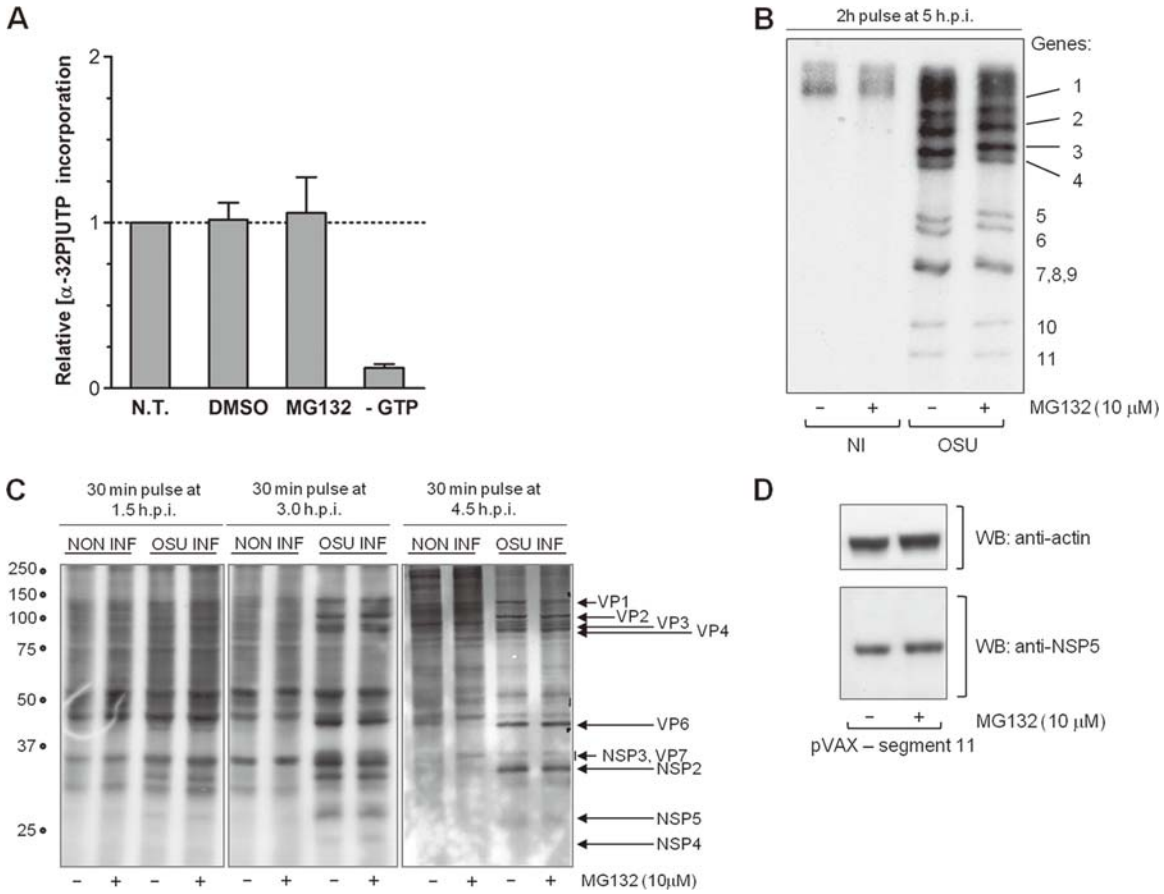

FIG. 5. Effect of proteasome inhibition on viral polymerase activities and production of viral proteins. (A) Transcriptase activity of DLPs. The plot shows the incorporation of [α-^{32}P]UTP into newly synthesized RNA from DLPs treated with DMSO or MG132 (10 μM) relative to incorporation from nontreated DLPs (N.T.). −GTP, negative control of transcription in the absence of GTP. Graph reports average ± standard error of the mean (SEM) of results from four different experiments. (B) Autoradiography of $^{32}P_i$-labeled viral dsRNAs from noninfected and virus-infected MA104 cells. Labeling and MG132 (10 μM) treatment were performed simultaneously from 5 h to 7 h p.i. (C) Autoradiography of [^{35}S]methionine-labeled viral proteins (30-min pulse at the indicated times p.i.) derived from OSU-infected or noninfected MA104 cells and treated or nontreated with MG132. (D) Western blot of extracts of BSRT7/5 cells transfected with a plasmid encoding the full-length virus-like mRNA sequence of gene 11 and treated or nontreated for 4 h with MG132 (10 μM), 20 h after transfection. Blots were reacted with the indicated antibodies; actin was used as a loading control; the hamster p53 is not detected by the anti-human p53 monoclonal antibody (MAb).

the beginning of each treatment, strongly suggesting that inhibition of proteasome activity affected the assembly of new viroplasms and their growth.

This was in fact confirmed by silencing, through RNA interference, genes encoding two proteasomal subunits (the ATPase subunits 1 and 6) that are essential for proteasome activity (21, 49) and the gene encoding the ubiquitin-ribosome protein S27 (RPS27) in order to reduce the levels of free ubiquitin and polyubiquitinylated proteins in the cytoplasm (22). Two siRNAs, specific for NSP5 of each strain, were used as controls of inhibited rotavirus replication (8). As shown in Fig. 8, silencing of the proteasomal subunits and RPS27 strongly affected accumulation of rotavirus proteins (Fig. 8A) and viroplasm formation (Fig. 8C). The impairment obtained with the C1 and C6 siRNAs treatment was similar to that observed with MG132, producing a comparable increase of p53 levels. The effectiveness of the siRNA for the C6 subunit was confirmed by Western blotting, as shown in Fig. 8B. Despite affecting significantly rotavirus replication, silencing of RPS27 was not effective in terms of variation of the p53 levels. This may be due to the facts that proteasome degradation of p53 is not exclusively dependent on ubiquitinylation (20) and that removing only one of the ubiquitin precursors may not be sufficient to reduce p53 ubiquitinylation. On the contrary, it has been reported that even a partial silencing of RPS27 can interfere with the replication cycle of other viruses (46). All these data further confirmed that a functional proteasome is required for rotavirus replication. It should be noted that, in spite of the strong effect on the formation of viroplasms, proteasome inhibition did not affect the ability of NSP5 to assemble into viroplasm-like structures (VLS) (10) formed upon coexpression with NSP2 and/or VP2 (Fig. 9). These observations suggest that inhibition of proteasomal activity does not alter the capacity of NSP5 to interact with either NSP2 or VP2 or its hyperphosphorylation induced by either of them (Fig. 6A).

Effect of proteasome inhibition on rotavirus does not depend on IFN-β levels. Previous reports have linked proteaso-

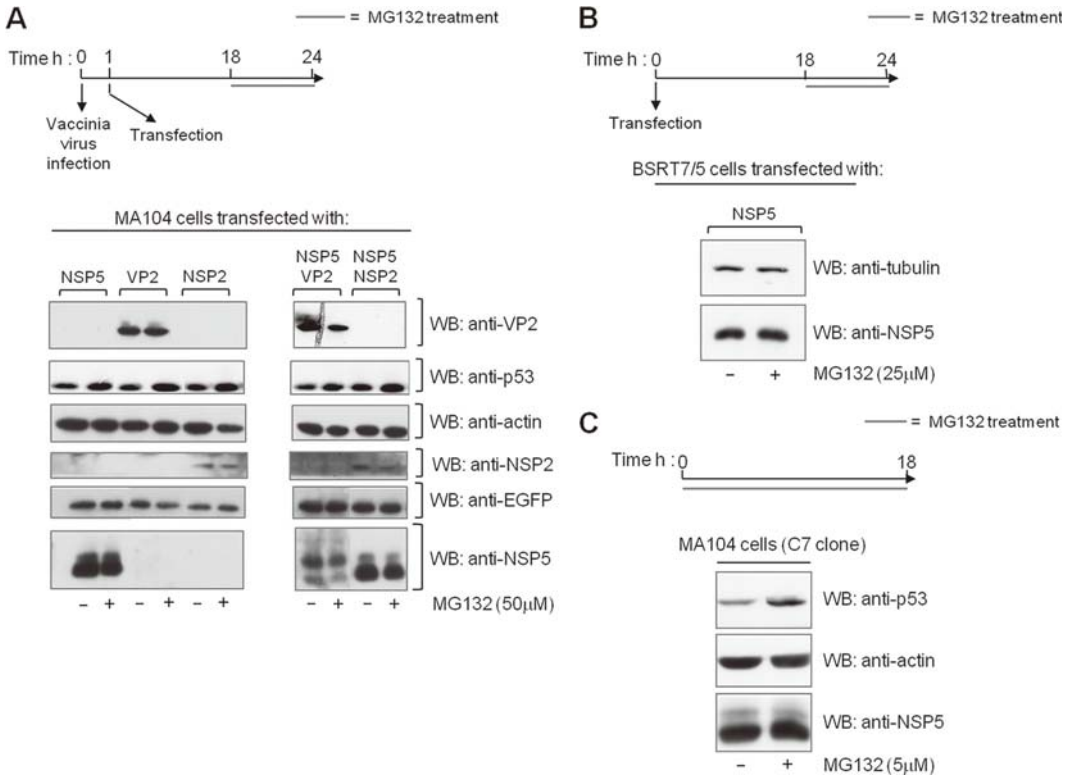

FIG. 6. Effect of proteasome inhibition on expression of transfected rotavirus proteins. (A) Western blot of extracts of MA104 cells infected with vaccinia virus and transfected with NSP5, VP2, and NSP2 genes, as indicated. Cells were lysed at 23 h posttransfection, following 6 h of MG132 or DMSO treatment. Blots were reacted with the indicated antibodies; transiently cotransfected EGFP gene was used as a transfection control, p53 was used to monitor proteasome inhibition, and actin was used as a loading control. (B) Western blot of extracts of BSRT7/5 cells transfected with NSP5 gene. Cells were lysed at 24 h posttransfection, following 6 h of MG132 or DMSO treatment. (C) Western blot of extracts of C7-MA104 cells following 18 h of MG132 or DMSO treatment.

mal activity to rotavirus infection in two different ways. In SA11-infected cells, it has been shown that the type I IFN response is antagonized by the virus through the viral protein NSP1, which drives proteasome-dependent degradation of IRF3, IRF5, and IRF7 (6, 7). In the OSU strain, however, IRF3 is not degraded upon infection, but NSP1 was described to inhibit activation of NFκB by inducing proteasome-dependent degradation of β-TrCP, the ubiquitin E3 ligase responsible for degradation of IκB, the NFκB inhibitor (26).

Since the SA11 and OSU strains were equally sensitive, we wanted to investigate whether the observed effect of proteasome inhibition on rotavirus replication was due to a premature activation of the IFN response. We first analyzed the levels of IRF3 in MG132-treated and untreated cells that were uninfected or infected with either rotavirus strain. The results showed no changes in IRF3 levels following infection with OSU, as expected (6, 7, 27), while infection with SA11 caused almost complete IRF3 degradation and partial recovery following MG132 treatment (Fig. 10B). Basal IRF3 levels in mock-infected cells were not affected by MG132 (Fig. 10B). Furthermore, as shown in Fig. 10C, quantitative real-time RT-PCR of IFN-β mRNA showed no significant changes following infection of MA104 cells by SA11 or OSU, in either the presence or the absence of MG132.

These data support the hypothesis that the interferon response is not related to the impaired rotavirus replication in the presence of proteasome inhibitors. Moreover, the stronger effect of MG132 on virus replication in OSU-infected cells, with higher IRF3 levels, further supports this interpretation.

DISCUSSION

The proteasomal degradation pathway of proteins is an essential cellular mechanism involved in a variety of different functions, such as regulation of gene expression, cell differentiation, control of cell cycle progression, and immune responses (32). In viral infections, the proteasome system is central for the production of peptides derived from viral proteins, which, upon loading on major histocompatibility complex (MHC) class I molecules and presentation on the cell surface, can become targets for cytotoxic T cells, resulting in the elimination of infected cells (29, 32).

Viruses have been shown to manipulate the ubiquitin-proteasome pathway at different stages of their life cycles, to enhance viral activities and/or to escape the antiviral cellular responses. For example, influenza virus has been shown to utilize the UPS for efficient trafficking to the late endosome/lysosome stages of virus entry (33), and recently it has been demonstrated that inhibition of proteasome activity affects influenza virus infection at a postfusion step (56); UPS also plays an important role in multiple steps of the coronavirus (CoV) infection cycle from viral entry to RNA synthesis (46). Also, in

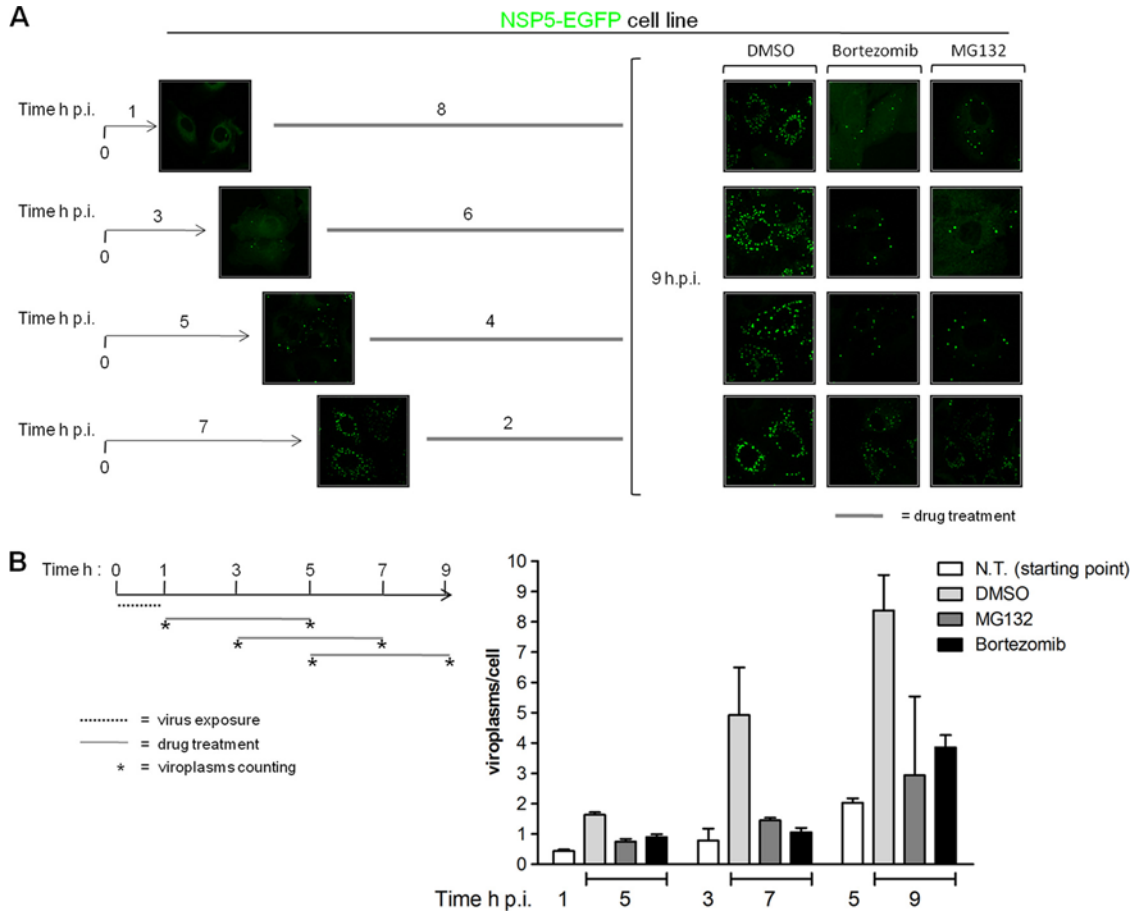

FIG. 7. Effect of proteasome activity on viroplasm formation. (A) Fluorescence analysis of viroplasm formation on NSP5-EGFP cells infected with rotavirus (OSU; MOI, 3) and treated or not treated with MG132 (10 μM) or bortezomib (10 μM) at different times p.i., as indicated. Cells were analyzed at the starting points (1 h, 3 h, 5 h, 7 h) and endpoints (9 h) of the inhibitor's window treatment. Single optical sections are shown. (B) Quantification of the accumulation of viroplasms in infected NSP5-EGFP/MA104 cells. At different times p.i., cells were treated for 4 h with DMSO or the indicated proteasome inhibitor and the number of viroplasms/cell was quantified at the starting (1 h, 3 h, 5 h; white bars) and endpoints (5 h, 7 h, 9 h) of treatment, indicated in the experimental scheme by an asterisk. N.T., nontreated. The graph shows the results from one representative experiment. Averages ± standard error of the means (SEM) are indicated in each column.

retroviruses, like HIV, a functional UPS is needed for the release of mature viral particles (31, 40). Among DNA viruses, multiple members of the *Herpesviridae* family have developed different strategies to manipulate UPS, such as encoding ubiquitin ligase-like proteins in order to target for degradation-specific host proteins (11, 34, 44), such as MHC class I molecules, to evade cytotoxic T cells. The parvovirus MVM (minute virus of mice) was also shown to use the proteasome machinery for facilitating its trafficking to the nucleus (48).

In this study, we have characterized the role of the proteasomal activity on the rotavirus replicative cycle. We found that inhibition of the proteasome blocked rotavirus replication, indicating that a functional proteasome is required for the virus to establish a productive replication cycle. Proteasome inhibition was effective in antagonizing the replication of three different rotavirus strains: simian SA11, porcine OSU, and bovine RF (data not shown).

In most experiments, we monitored virus replication, determining the production of viral proteins and in particular NSP5, whose expression is absolutely required for viral replication (8, 38, 55).

We show that an active proteasome is required during the early steps after entry and uncoating. Addition of the proteasome inhibitors MG132 or bortezomib after virus adsorption and entry (1 h) or even at 3 h p.i. had a strong impact on virus yields. In contrast, the presence of MG132 only during the attachment/adsorption and its subsequent removal still allowed a significant level of virus infection. In fact, the stronger effect was obtained when proteasome inhibition took place at relatively early time points up to 5 h p.i. (with a stronger effect for MG132 than for bortezomib), while inhibition at later time points (from 7 h to 10 h p.i.) had a weaker effect.

The main alteration found upon proteasome inhibition was a profound effect on the formation of viroplasms and their growth. This was more evident at early time points p.i. Indeed, when proteasome inhibitors were added, for instance, at 7 h p.i., the effect was no longer appreciable. Quantification of the effect showed that proteasome inhibition does not compromise

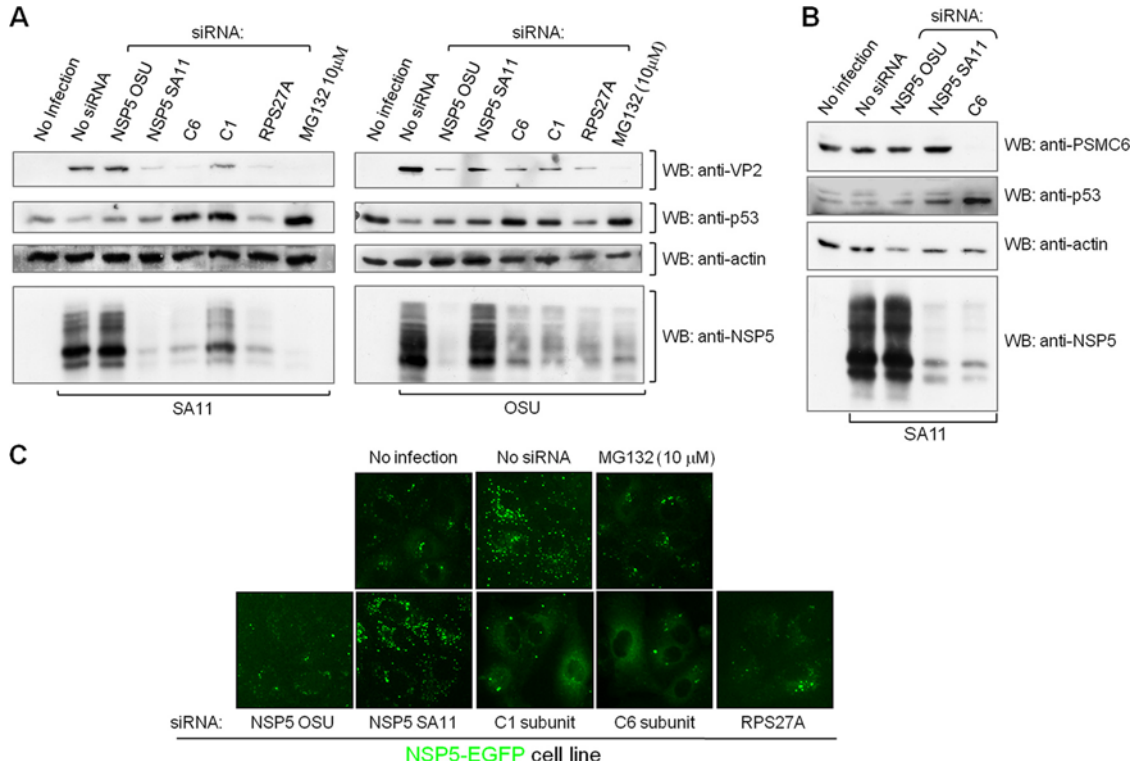

FIG. 8. Effect of silencing proteasomal subunits and ubiquitin precursor on rotavirus replication. (A) Western blot of cellular extracts of MA104 cells transfected with the indicated siRNAs and SA11 or OSU infected for 6 h, at day 2 after transfection. As a control, MG132 was added during the infection period. Blots were reacted with the indicated antibodies; p53 was used to monitor inhibition of the proteasome, and actin was used as a loading control. (B) Western blot as in panel A (left panel) showing strong silencing of the proteasomal C6 subunit. (C) Representative fluorescence images of viroplasms in OSU-infected NSP5-EGFP/MA104 cells, transfected with different siRNAs or treated with MG132, as indicated. The OSU- and SA11-specific siRNAs directed to NSP5 of each strain are used as controls.

the stability of viroplasms, since the number of viroplasms per cell remains essentially unchanged from the moment of addition of the inhibitor for a period of 5 to 7 h. Since the effect on viroplasm formation was observed almost immediately following the addition of the inhibitors, it could be hypothesized that the proteasomal activity is required for the degradation of a protein or a protein complex with a very short half-life.

The need of an active proteasome, suggested by the similar effects obtained with proteasome inhibitors with distinct mechanisms of action, such as MG132, bortezomib, and lactacystin (although not all of them with the same activity), was further confirmed by using siRNAs specific for two different proteasomal ATPase subunits (subunit 1 encoded by the PSMC1 gene and subunit 6 encoded by the PSMC6 gene) and for the ribosomal protein RPS27A, one of the main sources of ubiquitin. All three siRNAs had a strong effect on the replication of SA11 and OSU, although silencing of PSMC1 had a less pronounced effect on SA11.

RT-PCR analysis of virus-infected cells revealed that the amount of total viral RNAs (both mRNA and dsRNA) was heavily impaired upon treatment with MG132 for different times or at different time points p.i. However, the improbable direct effect of the inhibitors on the transcriptase and replicase activities of the viral polymerase VP1 was ruled out by determining *in vitro* the transcriptase activity of purified DLPs and *in vivo* the incorporation of $^{32}P_i$ into newly synthesized dsRNA. Using these two assays, we could distinguish putative effects on the two VP1 activities. These results suggested that the blockage was at a different level, most likely related to the degradation activity of the proteasome. This activity, however, does not appear to be related to the translation of viral proteins. Indeed, the rate of viral protein synthesis was not impaired by the addition of proteasome inhibitors even when they were added at very early time points p.i., suggesting that inhibition of viral protein synthesis following cellular stress is not involved. In this context, rotavirus infection has been shown to prevent the formation of stress granules despite the induction of eIF2α phosphorylation (41).

As recently described, transient expression of NSP5 with NSP2 and/or VP2 induces the formation of VLS in the cytosol (10). VLS formation, however, was not affected by proteasome inhibition, indicating that the events leading to the interaction of these three proteins *in vivo* do not depend on the proteasome activity. Furthermore, colocalization of other viral proteins into VLS (such as VP1 and VP6) was not altered (data not shown), suggesting that the interactions that allow VLS formation and recruitment of the viral constituents of the viroplasm can take place even when the proteasome is inhibited. The difference in sensitivities of viroplasms and VLS to proteasome inhibition, however, suggests that the similarities between them are mainly structural.

The data presented support the hypothesis that during in-

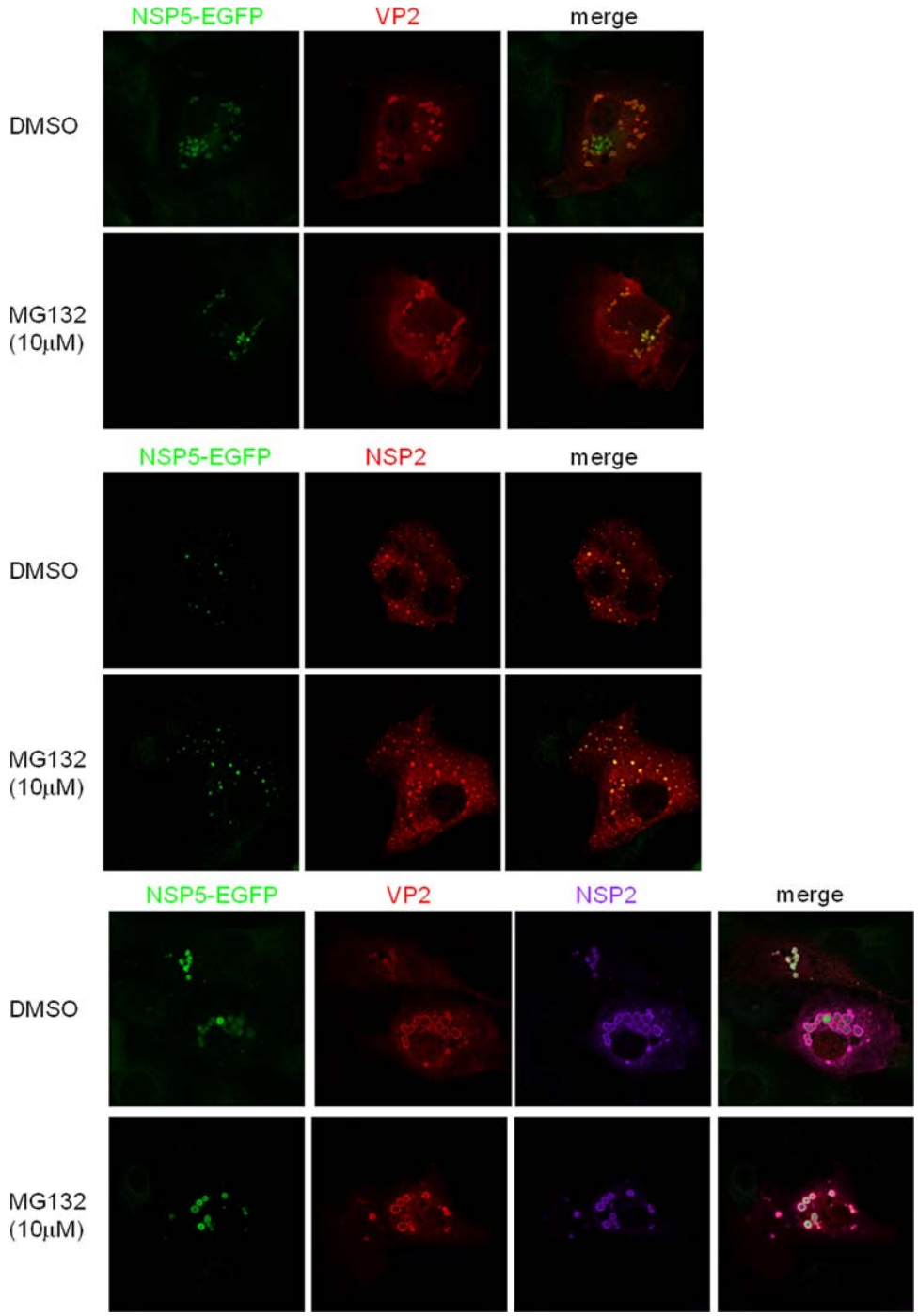

FIG. 9. Effect of proteasome inhibition on VLS formation. Confocal immunofluorescence of NSP5-EGFP/MA104 cells transfected with VP2 (red, upper panel) or NSP2 (red, middle panel), or with both NSP2 (purple) and VP2 (red) in the bottom panel, and treated with MG132 or DMSO. Cells were infected with vaccinia virus 1 h before transfection and treated with MG132 at 23 h posttransfection for 6 h.

fection, an unidentified proteasome-sensitive host factor capable of impairing, either directly or indirectly, formation of viroplasms needs to be removed in order to sustain active virus replication. Once assembled, however, viroplasms are not affected by proteasome inhibition, as they continue to be present after several hours of treatment. Interestingly, whatever the factor responsible for the blockage, it appears not to affect the formation of VLS, thus suggesting a function related to either recruitment of some cellular protein(s) relevant for the assembly of viroplasms or, alternatively, the recruitment of viral RNA templates for the synthesis of dsRNA.

We investigated the possible involvement of an enhanced IFN-β production as a consequence of proteasome inhibition. Different mechanisms of antagonizing induction of IFN-β have

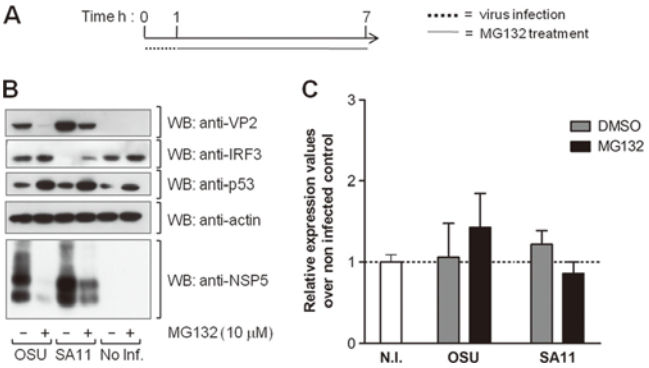

FIG. 10. Proteasome inhibition and IFN-β induction. (A) Schematic representation of the experiments shown in B and C, performed on virus-infected MA104 cells. (B) Western blot showing IRF3 levels in extracts from MG132-treated and nontreated cells. Blots were reacted with the indicated antibodies; p53 was used to monitor proteasome inhibition, and actin was used as a loading control. (C) Quantitative RT-PCR of IFN-β mRNA in uninfected or SA11- and OSU-infected cells in the presence or absence of MG132.

been described depending on cell type and rotavirus strain (13, 50, 51). In particular, in SA11-infected cells IRF3 interacts with NSP1 and as a consequence is degraded in a proteasomal-dependent way, thus impairing activation of IFN-β gene transcription (6). NSP1 of strain OSU, instead, does not induce degradation of IRF3 but blocks proteasomal degradation of IκB, with the consequent retention of NFkB p65 in the cytosol (26, 30). We show that in cells infected by both virus strains the IFN-β levels remained unaltered upon proteasome inhibition, despite the partial recovery of IRF3 levels in SA11-infected cells treated with MG132. We thus concluded that the impaired viral replication upon proteasome inhibition was not the consequence of an enhanced IFN-β level. However, since it has recently been described that active translocation of NFκB p65 into the nucleus of SA11-infected cells, rather than inducing IFN-β transcription, functions as an anti-apoptotic signal to prolong survival of host cells (5), we cannot rule out that activation of factors involved in apoptotic pathways are linked to the effects of proteasome inhibition on virus replication.

Impairment of viral infection by proteasome inhibitors has been recently described for two other dsRNA viruses, the avian reovirus ARV (9) and the infectious bursal disease virus IBDV (36). In these two viruses, inhibition of the proteasome causes a reduction in the production of viral progeny with an evident effect at the early phases of infection, suggesting a possible common mechanism of involvement of the UPS. The data indicate that rotaviruses, like other viruses, are adapted to replicate in cellular environments with active proteasomal activity.

Moreover, the data suggest that manipulation of proteasome activity may be used as a therapeutic approach to contain rotaviral infection. In this context, it is noteworthy that proteasome inhibition impaired coronavirus replication in *in vitro* infected cells while *in vivo* administration did not have a positive effect in controlling infection (45, 46); the opposite was reported for coxsackievirus to control development of myocarditis in mice (24).

ACKNOWLEDGMENTS

R.C. was supported by the ICGEB predoctoral fellowship of the Corso di Perfezionamento of the Scuola Normale Superiore di Pisa. F.A. was partially supported by a postdoctoral fellowship from the Area Science Park of Trieste, Italy, and by a FIRB project funded by the Ministero dell'Istruzione, dell'Università e della Ricerca, Italy. M.M. was supported by Project SeND—Search for New Drugs, funded by Region Friuli Venezia Giulia, and 3rd supplementary contract of Framework Programme on Scientific Research of the Regione Friuli Venezia Giulia, Italy.

We acknowledge K. Conzelmann (Ludwig-Maximilians-Universität, Munich, Germany) for the BSRT7-5 cell line. We are indebted to Fabio Rossi for helpful discussions.

REFERENCES

1. **Afrikanova, I., E. Fabbretti, M. C. Miozzo, and O. R. Burrone.** 1998. Rotavirus NSP5 phosphorylation is up-regulated by interaction with NSP2. J. Gen. Virol. **79**(pt. 11)**:**2679–2686.
2. **Afrikanova, I., M. C. Miozzo, S. Giambiagi, and O. Burrone.** 1996. Phosphorylation generates different forms of rotavirus NSP5. J. Gen. Virol. **77**(pt. 9)**:**2059–2065.
3. **Altenburg, B. C., D. Y. Graham, and M. K. Estes.** 1980. Ultrastructural study of rotavirus replication in cultured cells. J. Gen. Virol. **46:**75–85.
4. **Arnoldi, F., M. Campagna, C. Eichwald, U. Desselberger, and O. R. Burrone.** 2007. Interaction of rotavirus polymerase VP1 with nonstructural protein NSP5 is stronger than that with NSP2. J. Virol. **81:**2128–2137.
5. **Bagchi, P., D. Dutta, S. Chattopadhyay, A. Mukherjee, U. C. Halder, S. Sarkar, N. Kobayashi, S. Komoto, K. Taniguchi, and M. Chawla-Sarkar.** 2010. Rotavirus nonstructural protein 1 suppresses virus-induced cellular apoptosis to facilitate viral growth by activating the cell survival pathways during early stages of infection. J. Virol. **84:**6834–6845.
6. **Barro, M., and J. T. Patton.** 2005. Rotavirus nonstructural protein 1 subverts innate immune response by inducing degradation of IFN regulatory factor 3. Proc. Natl. Acad. Sci. U. S. A. **102:**4114–4119.
7. **Barro, M., and J. T. Patton.** 2007. Rotavirus NSP1 inhibits expression of type I interferon by antagonizing the function of interferon regulatory factors IRF3, IRF5, and IRF7. J. Virol. **81:**4473–4481.
8. **Campagna, M., C. Eichwald, F. Vascotto, and O. R. Burrone.** 2005. RNA interference of rotavirus segment 11 mRNA reveals the essential role of NSP5 in the virus replicative cycle. J. Gen. Virol. **86:**1481–1487.
9. **Chen, Y. T., C. H. Lin, W. T. Ji, S. K. Li, and H. J. Liu.** 2008. Proteasome inhibition reduces avian reovirus replication and apoptosis induction in cultured cells. J. Virol. Methods **151:**95–100.
10. **Contin, R., F. Arnoldi, M. Campagna, and O. R. Burrone.**2010. Rotavirus NSP5 orchestrates recruitment of viroplasmic proteins. J. Gen. Virol. **91:** 1782–1793.
11. **Coscoy, L., D. J. Sanchez, and D. Ganem.** 2001. A novel class of herpesvirus-encoded membrane-bound E3 ubiquitin ligases regulates endocytosis of proteins involved in immune recognition. J. Cell Biol. **155:**1265–1273.
12. **Cuadras, M. A., B. B. Bordier, J. L. Zambrano, J. E. Ludert, and H. B. Greenberg.** 2006. Dissecting rotavirus particle-raft interaction with small interfering RNAs: insights into rotavirus transit through the secretory pathway. J. Virol. **80:**3935–3946.
13. **Douagi, I., et al.** 2007. Role of interferon regulatory factor 3 in type I interferon responses in rotavirus-infected dendritic cells and fibroblasts. J. Virol. **81:**2758–2768.
14. **Eichwald, C., J. F. Rodriguez, and O. R. Burrone.** 2004. Characterization of rotavirus NSP2/NSP5 interaction and dynamics of viroplasms formation. J. Gen. Virol. **85:**625–634.
15. **Eichwald, C., F. Vascotto, E. Fabbretti, and O. R. Burrone.** 2002. Rotavirus NSP5: mapping phosphorylation sites and kinase activation and viroplasm localization domains. J. Virol. **76:**3461–3470.
16. **Esparza, J., M. Gorziglia, F. Gil, and H. Romer.** 1980. Multiplication of human rotavirus in cultured cells: an electron microscopic study. J. Gen. Virol. **47:**461–472.
17. **Estes, M., and A. Kapikian.** 2007. Rotaviruses, p. 1917–1974. *In* D. M. Knipe, et al. (ed.), Fields virology, 5th ed. Wolters Kluwer Health/Lippincott Williams & Wilkins, Philadelphia, PA.
18. **Estes, M. K., D. Y. Graham, C. P. Gerba, and E. M. Smith.** 1979. Simian rotavirus SA11 replication in cell cultures. J. Virol. **31:**810–815.
19. **Fabbretti, E., I. Afrikanova, F. Vascotto, and O. R. Burrone.** 1999. Two non-structural rotavirus proteins, NSP2 and NSP5, form viroplasm-like structures in vivo. J. Gen. Virol. **80**(pt. 2)**:**333–339.
20. **Feng, L., T. Lin, H. Uranishi, W. Gu, and Y. Xu.** 2005. Functional analysis of the roles of posttranslational modifications at the p53 C terminus in regulating p53 stability and activity. Mol. Cell. Biol. **25:**5389–5395.
21. **Finley, D.** 2009. Recognition and processing of ubiquitin-protein conjugates by the proteasome. Annu. Rev. Biochem. **78:**477–513.
22. **Finley, D., B. Bartel, and A. Varshavsky.** 1989. The tails of ubiquitin pre-

cursors are ribosomal proteins whose fusion to ubiquitin facilitates ribosome biogenesis. Nature **338:**394–401.
23. **Fuerst, T. R., E. G. Niles, F. W. Studier, and B. Moss.** 1986. Eukaryotic transient-expression system based on recombinant vaccinia virus that synthesizes bacteriophage T7 RNA polymerase. Proc. Natl. Acad. Sci. U. S. A. **83:**8122–8126.
24. **Gao, G., et al.** 2008. Proteasome inhibition attenuates coxsackievirus-induced myocardial damage in mice. Am. J. Physiol. Heart Circ. Physiol. **295:**H401–H408.
25. **Gonzalez, S. A., and O. R. Burrone.** 1991. Rotavirus NS26 is modified by addition of single O-linked residues of N-acetylglucosamine. Virology **182:** 8–16.
26. **Graff, J. W., K. Ettayebi, and M. E. Hardy.** 2009. Rotavirus NSP1 inhibits NFkappaB activation by inducing proteasome-dependent degradation of beta-TrCP: a novel mechanism of IFN antagonism. PLoS Pathog. **5:**e1000280.
27. **Graff, J. W., J. Ewen, K. Ettayebi, and M. E. Hardy.** 2007. Zinc-binding domain of rotavirus NSP1 is required for proteasome-dependent degradation of IRF3 and autoregulatory NSP1 stability. J. Gen. Virol. **88:**613–620.
28. **Graham, A., G. Kudesia, A. M. Allen, and U. Desselberger.** 1987. Reassortment of human rotavirus possessing genome rearrangements with bovine rotavirus: evidence for host cell selection. J. Gen. Virol. **68**(pt. 1)**:**115–122.
29. **Hansen, T. H., and M. Bouvier.** 2009. MHC class I antigen presentation: learning from viral evasion strategies. Nat. Rev. Immunol. **9:**503–513.
30. **Holloway, G., T. T. Truong, and B. S. Coulson.** 2009. Rotavirus antagonizes cellular antiviral responses by inhibiting the nuclear accumulation of STAT1, STAT2, and NF-kappaB. J. Virol. **83:**4942–4951.
31. **Isaacson, M. K., and H. L. Ploegh.** 2009. Ubiquitination, ubiquitin-like modifiers, and deubiquitination in viral infection. Cell Host Microbe **5:**559–570.
32. **Jung, T., B. Catalgol, and T. Grune.** 2009. The proteasomal system. Mol. Aspects Med. **30:**191–296.
33. **Khor, R., L. J. McElroy, and G. R. Whittaker.** 2003. The ubiquitin-vacuolar protein sorting system is selectively required during entry of influenza virus into host cells. Traffic **4:**857–868.
34. **Kikkert, M., et al.** 2001. Ubiquitination is essential for human cytomegalovirus US11-mediated dislocation of MHC class I molecules from the endoplasmic reticulum to the cytosol. Biochem. J. **358:**369–377.
35. **Lawton, J. A., M. K. Estes, and B. V. Prasad.** 1997. Three-dimensional visualization of mRNA release from actively transcribing rotavirus particles. Nat. Struct. Biol. **4:**118–121.
36. **Liu, J., L. Wei, T. Jiang, L. Shi, and J. Wang.** 2007. Reduction of infectious bursal disease virus replication in cultured cells by proteasome inhibitors. Virus Genes **35:**719–727.
37. **Lopez, T., et al.** 2005. Silencing the morphogenesis of rotavirus. J. Virol. **79:**184–192.
38. **Lopez, T., M. Rojas, C. Ayala-Breton, S. Lopez, and C. F. Arias.** 2005. Reduced expression of the rotavirus NSP5 gene has a pleiotropic effect on virus replication. J. Gen. Virol. **86:**1609–1617.
39. **Maki, C. G., J. M. Huibregtse, and P. M. Howley.** 1996. In vivo ubiquitination and proteasome-mediated degradation of p53(1). Cancer Res. **56:**2649–2654.
40. **Martin-Serrano, J.** 2007. The role of ubiquitin in retroviral egress. Traffic **8:**1297–1303.
41. **Montero, H., M. Rojas, C. F. Arias, and S. Lopez.** 2008. Rotavirus infection induces the phosphorylation of eIF2alpha but prevents the formation of stress granules. J. Virol. **82:**1496–1504.
42. **Petrie, B. L., H. B. Greenberg, D. Y. Graham, and M. K. Estes.** 1984. Ultrastructural localization of rotavirus antigens using colloidal gold. Virus Res. **1:**133–152.
43. **Prasad, B. V., G. J. Wang, J. P. Clerx, and W. Chiu.** 1988. Three-dimensional structure of rotavirus. J. Mol. Biol. **199:**269–275.
44. **Prosch, S., et al.** 2003. Proteasome inhibitors: a novel tool to suppress human cytomegalovirus replication and virus-induced immune modulation. Antivir. Ther. **8:**555–567.
45. **Raaben, M., G. C. Grinwis, P. J. Rottier, and C. A. de Haan.** The proteasome inhibitor Velcade enhances rather than reduces disease in mouse hepatitis coronavirus-infected mice. J. Virol. **84:**7880–7885.
46. **Raaben, M., C. C. Posthuma, M. H. Verheije, E. G. te Lintelo, et al.** The ubiquitin-proteasome system plays an important role during various stages of the coronavirus infection cycle. J. Virol. **84:**7869–7879.
47. **Randow, F., and P. J. Lehner.** 2009. Viral avoidance and exploitation of the ubiquitin system. Nat. Cell Biol. **11:**527–534.
48. **Ros, C., and C. Kempf.** 2004. The ubiquitin-proteasome machinery is essential for nuclear translocation of incoming minute virus of mice. Virology **324:**350–360.
49. **Rubin, D. M., M. H. Glickman, C. N. Larsen, S. Dhruvakumar, and D. Finley.** 1998. Active site mutants in the six regulatory particle ATPases reveal multiple roles for ATP in the proteasome. EMBO J. **17:**4909–4919.
50. **Sen, A., N. Feng, K. Ettayebi, M. E. Hardy, and H. B. Greenberg.** 2009. IRF3 inhibition by rotavirus NSP1 is host cell and virus strain dependent but independent of NSP1 proteasomal degradation. J. Virol. **83:**10322–10335.
51. **Sherry, B.** 2009. Rotavirus and reovirus modulation of the interferon response. J. Interferon Cytokine Res. **29:**559–567.
52. **Silvestri, L. S., Z. F. Taraporewala, and J. T. Patton.** 2004. Rotavirus replication: plus-sense templates for double-stranded RNA synthesis are made in viroplasms. J. Virol. **78:**7763–7774.
53. **Spencer, E., and M. L. Arias.** 1981. In vitro transcription catalyzed by heat-treated human rotavirus. J. Virol. **40:**1–10.
54. **Stacy-Phipps, S., and J. T. Patton.** 1987. Synthesis of plus- and minus-strand RNA in rotavirus-infected cells. J. Virol. **61:**3479–3484.
55. **Vascotto, F., M. Campagna, M. Visintin, A. Cattaneo, and O. R. Burrone.** 2004. Effects of intrabodies specific for rotavirus NSP5 during the virus replicative cycle. J. Gen. Virol. **85:**3285–3290.
56. **Widjaja, I., et al.** 2010. Inhibition of the ubiquitin-proteasome system affects influenza A virus infection at a postfusion step. J. Virol. **84:**9625–9631.
57. **Yeager, M., K. A. Dryden, N. H. Olson, H. B. Greenberg, and T. S. Baker.** 1990. Three-dimensional structure of rhesus rotavirus by cryoelectron microscopy and image reconstruction. J. Cell Biol. **110:**2133–2144.